

Research Article

Oxidation/Corrosion Behaviour of ODS Ferritic/Martensitic Steels in Pb Melt at Elevated Temperature

O. I. Yaskiv and V. M. Fedirko

Institute for Physics and Mechanics of National Academy of Sciences of Ukraine, 5 Naukova Street, Lviv 79601, Ukraine

Correspondence should be addressed to O. I. Yaskiv; oleh.yaskiv@ipm.lviv.ua

Received 12 December 2013; Revised 31 January 2014; Accepted 31 January 2014; Published 3 March 2014

Academic Editor: Massimo Zucchetti

Copyright © 2014 O. I. Yaskiv and V. M. Fedirko. This is an open access article distributed under the Creative Commons Attribution License, which permits unrestricted use, distribution, and reproduction in any medium, provided the original work is properly cited.

Lead-based melts (Pb, Pb-Bi) are considered as candidate coolants and spallation neutron targets due to their excellent thermophysical and nuclear properties. However, the corrosion of structural materials remains a major issue. Oxide dispersion strengthened (ODS) ferritic/martensitic steels are considered for high temperature application for both fission and fusion reactor concepts. The oxidation/corrosion kinetics in a static oxygen-saturated Pb melt at temperature of 550°C as well as the morphology and composition of scales formed on ferritic/martensitic Fe-9Cr-1.5W and ferritic Fe-14Cr-1.5W ODS steels have been investigated. Both materials showed homogeneous multiple, dense scales that consisted of typical combination of Fe₃O₄ as outer sublayer and (Fe,Cr)₃O₄ as inner sublayer. A nonuniform growth of inner oxide sublayers into the metal matrix as well as a good adhesion to the metal substrate is observed. With the prolongation of exposure from 240 to 1000 h, observed scales grow from 35 μm to 45 μm for ODS Fe-9Cr steel and from 40 μm to 60 μm for ODS Fe-14Cr steel with the thinning rates of 0,22 and 0,31 mm/year correspondingly. The mechanism of scales formation is discussed.

1. Introduction

Lead-based melts (Pb, Pb-Bi) are considered for use in Generation IV reactor coolant and spallation neutron targets due to their excellent thermophysical and nuclear properties [1]. The advantage of lead as a nuclear coolant is derived from its physical and chemical properties [2]. At the same time, the corrosion aggressiveness of lead melts with regard to the structural materials is one of the main issues of up-to-date reactor material science [3]. To make this system usable at high temperatures (above 500°C), new classes of materials need to be developed and studied.

Oxide dispersion strengthened (ODS) ferritic/martensitic steels are considered as candidate structure materials for high temperature application for both fission (Generation IV, Accelerator Driven Systems—ADS) and fusion reactor concepts [4, 5]. Their properties (high temperature strength and creep resistance) make them potentially usable for high temperature application in liquid metal cooled systems [6]. Although an application of

ODS steels allows the working temperature limit to be increased up to about 700°C, it is known that the corrosion aggressiveness of liquid metals regarding steels strongly depends on temperature; that is, the higher the temperature, the larger corrosion losses [7, 8]. In addition to the temperature, the specific phase-structural state of ODS steels, that is, presence of dispersion oxide particles (TiO₂ and/or Y₂O₃) as well as fine-grained structure with high length of structural boundaries and residual porosity can substantially influence the intensity of corrosion interaction [9]. Therefore, the compatibility of ODS steels with lead melts at elevated temperatures is one of the most important issues of up-to-date nuclear investigations.

It is well known also that the quality of oxide layer depends, in general, on the level of oxidation potential of the melt and composition and surface structure of the steel. Therefore, it is very important to understand the effect of specific structure of ODS steels (dispersive oxide particles and fine-grained structure) on corrosion processes in Pb-based melts.

The aim of present paper was to investigate the oxidation/corrosion behavior of ferritic and ferritic/martensitic ODS steels in static oxygen-saturated Pb melt at elevated temperature.

2. Experiment

The samples ($\text{Ø}10 \text{ mm} \times 3 \text{ mm}$) were prepared from ferritic/martensitic Fe-9Cr-1.5W and ferritic Fe-14Cr-1.5W ODS steels (strengthened with Y_2O_3).

Before investigations, samples were polished and thermally vacuum-treated at 1100°C for 1 h.

A glove box allowing work with the highly reactive liquid metals (Li, Pb-Li, Pb, Bi, etc.) with using an argon neutral gas atmosphere, equipped with the heating and welding devices, was used to set samples into crucible.

Corrosion tests were performed in isothermal static oxygen-saturated Pb melt ($C_{\text{O}[\text{Pb}]} \sim 10^{-3} \text{ wt\% O}$) at 550°C for exposures 240 h, 500 h, and 1000 h. Samples were fixed in alumina crucibles, then filled with melt, placed in the furnace, and tested for the required time. To provide the oxygen-saturated conditions, the liquid metal was in contact with dry air during the test and therefore the red-colored PbO oxide scale was formed separating gas and liquid metal phases. Lead oxide indicates that the oxygen concentration in the melt (beneath the PbO oxide scale) is equal to the equation $\lg C_{\text{O}[\text{Pb}]} = 3.2 - 5000/T$, averaged $\sim 10^{-3} \text{ wt\% O}$ and melt was in oxygen-saturated conditions.

When tested, the samples were quickly extracted from the melt and cooled to save high-temperature state of scales. Some samples were cleaned in 1/3 ethanol, 1/3 acetic acid, and 1/3 hydrogen peroxide mixture (1:1:1) at room temperature to remove adhered Pb from the surface.

A scanning electron microscope (SEM), Carl Zeiss AG-EVO 40 Series equipped with the Energy-dispersive X-ray spectrometer, was used to observe the morphology and composition of oxide layers as well as the oxidation kinetics.

3. Results

3.1. Morphology of Scales

3.1.1. Fe-9Cr. The cross-sectional SEM measurement of Fe-9Cr ODS steel after 240 h exposure to Pb-melt is given in Figure 1(a). There is a clear regularity in the increase of Cr from outer layer scale (about 0.8 wt.%) to inner layer scale (23.7 wt.%) (Figure 1(a), areas 1–4). A slight depletion of Fe from area 1 to area 4 is observed. This means that the outer sublayer (Figure 1(a), area 1) consists mainly of magnetite Fe_3O_4 , whereas the inner sublayers (Figure 1(a), areas 2–4) are enriched in Cr and consist of a spinel $(\text{Fe,Cr})_3\text{O}_4$. No cracks between the inner layer and the steel's substrate were observed. It should be noted that the Fe_3O_4 layer is not continuous and therefore it can be concluded that at this stage the process of magnetite formation begins. The concentration of the steel components below the oxide layer is unchanged.

The cross-sectional SEM measurement of steel after 500 h exposure is given in Figure 1(b). There are several sublayers

differed in Cr amount. Most likely, these layers may be identified as $(\text{Fe,Cr})_3\text{O}_4$ in which Cr changes from 4,5 wt.% in the outer sublayer to 14 wt.% in the inner sublayer. A clear boundary between the inner and outer layers was detected following 500 h lead exposure.

The cross-sectional SEM measurement of steel after 1000 h exposure is given in Figure 2. The front of the oxide scale is irregular, particularly the inner sublayer. Following prolonged exposure of 1000 h, two clearly separated sublayers are formed on the surface. The outer oxide layer consists of a slight amount of Cr (3,2% wt.%) (Figure 2, point 1) and can therefore be attributed as a magnetite Fe_3O_4 , whereas the inner sublayer consists of 22,8 wt.% Cr (Figure 2, point 2) and can therefore be considered as a spinel $(\text{Fe,Cr})_3\text{O}_4$.

Hence, it can be concluded that during exposure of Fe-9Cr ODS steel to oxygen-saturated Pb melt the Cr-enriched oxide scale consisting of two sublayers differing in Cr amounts is formed. With prolonged exposure, the outer sublayer transforms to Fe_3O_4 , whereas the inner layer remains unchanged $(\text{Fe,Cr})_3\text{O}_4$. No pitting formation or grain boundary oxidation was found. The inner sublayer is well adhered to the steel's substrate. A slight loss in outerlayer uniformity can be observed with prolonged exposure.

3.1.2. Fe-14Cr. When considering Fe-14Cr ODS steel, the kinetics of scale's growth is similar to those for Fe-9Cr ODS steel. The cross section of Fe-14Cr steel following exposure to Pb melt for 240 h is given in Figure 3. There are some regions differing with grey tint and one black colored sublayer in the scale's morphology. Grey colored areas correspond to $(\text{Fe,Cr})_3\text{O}_4$ oxide in which the Cr amount changes from 17 wt.% at the bottom (Figure 3, areas 1–3) to 27 wt.% at the top (Figure 3, area 5). The black colored sublayer consists of a negligible proportion of Cr, about 2 wt.% (Figure 3, area 4), which proves that this layer is composed of Fe_3O_4 . No continuous boundary of separated sublayers is observed.

The morphology and elemental composition of scale formed after 500 h exposure are shown in Figure 4. The front of the scale can be seen to grow irregularly. The grey-colored areas of inner sublayers (Figure 4, areas 2–4) correspond to Cr-enriched $(\text{Fe,Cr})_3\text{O}_4$ oxide (Cr is up to 29,5 wt.%), while the dark-grey colored area of outer sublayer is Cr-depleted (11 wt.%). This outer sublayer (Figure 4, area 1) may be attributed to Fe_3O_4 oxide. No selective oxidation like pitting or grain boundary oxidation was found. The inner sublayer is well bonded to the steel's substrate. As seen in Figure 4, the inner sublayer grows discontinuously and towards the metal matrix.

The front of the scale after 1000 h of exposure grows very irregularly (Figure 5). The cracks separating outer and inner sublayers are observed. The separated sections of the scale are also seen. The scale consists of magnetite and spinel $(\text{Fe,Cr})_3\text{O}_4$ with different amount of Cr. The outer sublayer is Cr-depleted (Figure 5, area 1) and consists of Fe_3O_4 , whereas the inner sublayers are Cr-enriched (up to 30 wt.%) (Figure 5, areas 2, 4, and 5).

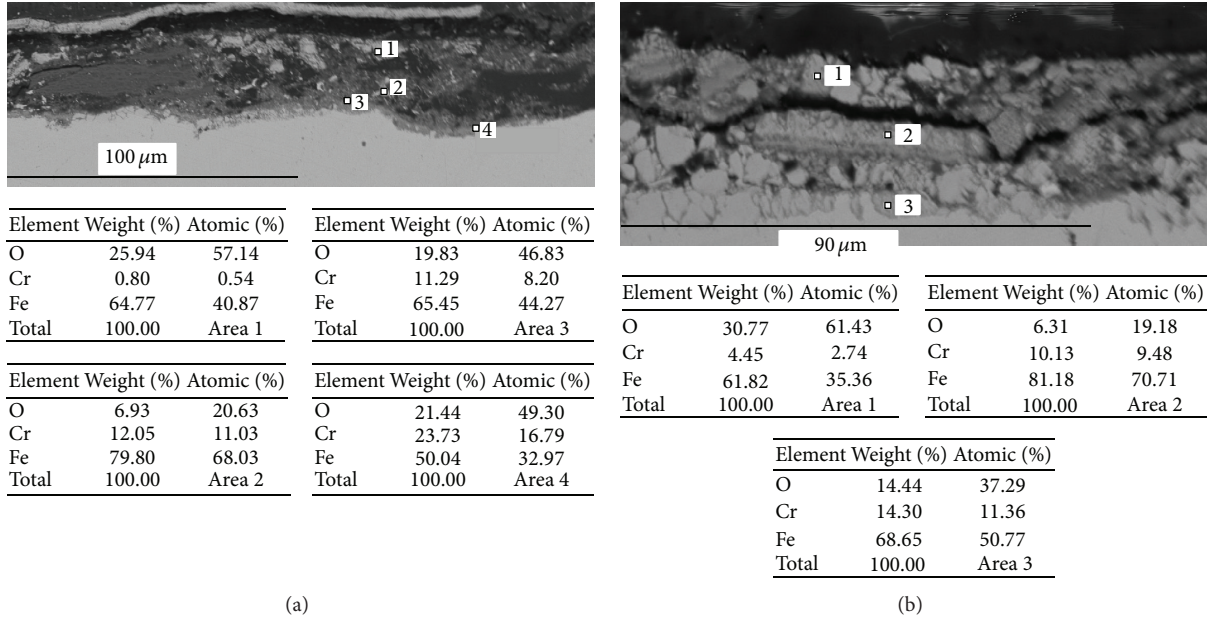


FIGURE 1: Morphology and elemental amount of scales formed on Fe-9Cr ODS steel after exposure to static oxygen-saturated Pb-melt at 550°C for (a) 240 h and (b) 500 h.

TABLE 1: The scale dimension (μm) and thinning of samples (mm/year) versus exposure time of Fe-9Cr and Fe-14Cr ODS steels facing the oxygen-saturated Pb melt at temperature 550°C.

Steel	Time, h	Thickness of scale, μm			Thinning, mm/year	Remarks
		Whole	Outer	Inner		
Fe-9Cr	240	35	10	25	—	Thin, compact, and dense oxide layer
	500	40	15	25	—	Thick, compact, and dense oxide layer
	1000	45	20	25	0.22	Thick, compact, and dense oxide layer
Fe-14Cr	240	45	15	30	—	Thin, compact, and dense oxide layer
	500	40	15	25	—	Thick, compact, and dense oxide layer
	1000	60	25	35	0.31	Thick, compact, and dense oxide layer

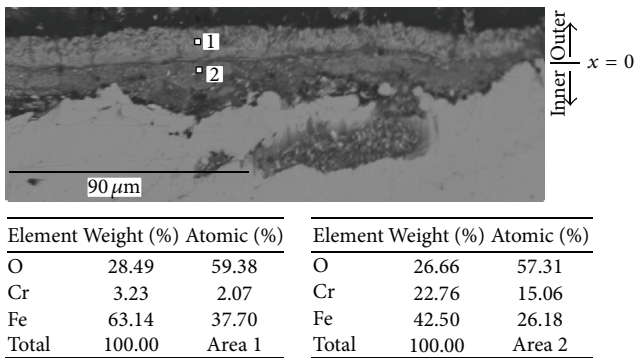


FIGURE 2: Morphology and elemental amount of scales formed on ODS Fe-9Cr steel after exposure to static oxygen-saturated Pb-melt at 550°C for 1000 h.

3.2. Oxidation Kinetics. The thickness of whole scales and their outer and inner sublayers as well as a short description of the appearance of the oxide scales of tested materials are presented in Table 1. As a rule, the inner sublayer has more

thickness as compared to outer sublayer. All scales observed were dense and were well adhered to the material substrate.

The average total thickness of oxide scale on Fe-9Cr slightly increases with exposure: from 35 μm for 240 h to 45 μm for 1000 h. The average total thickness of oxide scale on Fe-14Cr reaches 45 μm after 240–500 h. After 1000 h, the thickening of the scale up to 60 μm takes place.

The thinning of steel exposed to oxygen-saturated Pb melt for 1000 h can be estimated at a corrosion rate of 0.22 mm/year for Fe-9Cr steel and 0.31 mm/year for Fe-14Cr steel.

4. Discussion on Mechanism of Scale Formation

The presence of oxygen impurities in lead melts alters substantially the interaction between structural materials and melts from dissolution to oxidation [10, 11].

According to the thermodynamic evaluation, the main steel components (Fe and Cr) have higher affinity to oxygen than Pb [12]. Based on the phase state Fe-O diagram, iron

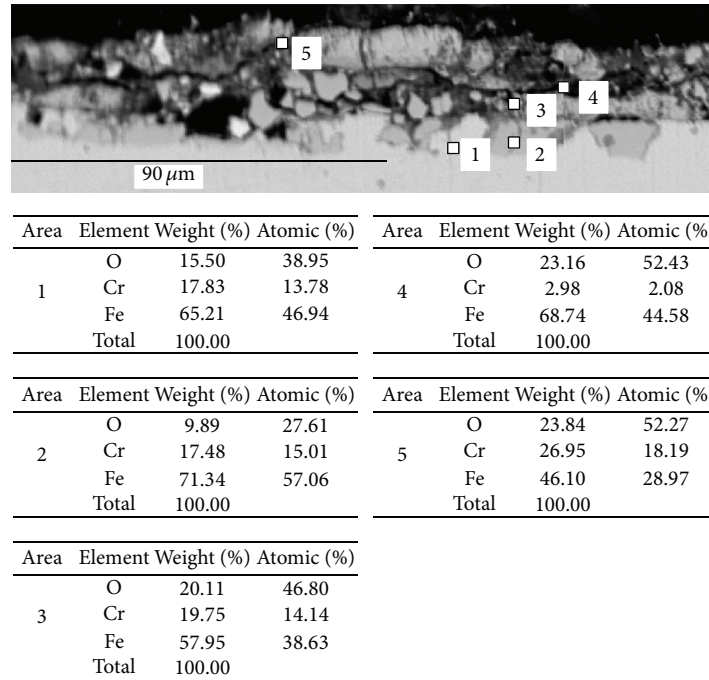


FIGURE 3: Morphology and elemental amount of scales formed on ODS Fe-14Cr steel after exposure to static oxygen-saturated Pb-melt at 550°C for 240 h.

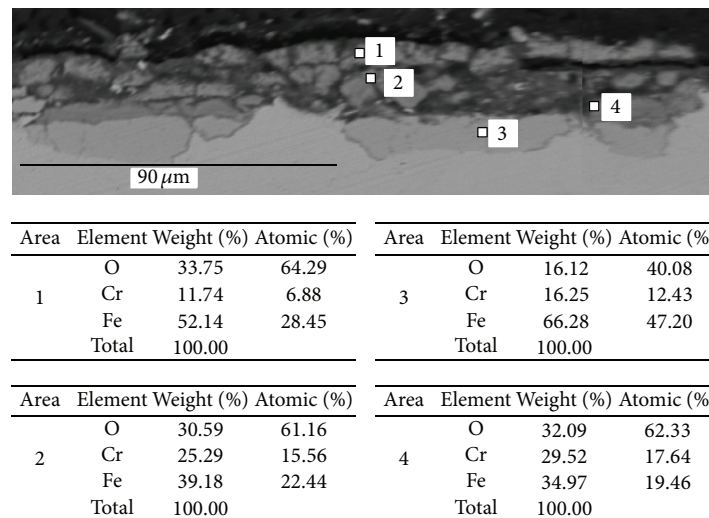


FIGURE 4: Morphology and elemental amount of scales formed on ODS Fe-14Cr steel after exposure to static oxygen-saturated Pb-melt at 550°C for 500 h.

can oxidize at $T > 570^\circ\text{C}$ to form magnetite and wustite (Fe_3O_4 and FeO accordingly), while at $T < 570^\circ\text{C}$ magnetite is the prevailing phase. Y_2O_3 oxide particles presented as a strengthened agent in ODS steels should be stable in the Pb melt under given conditions of liquid metal with respect to the oxygen concentration [13].

Since an affinity of the main steel's components (Fe and Cr) to the oxygen is higher than that of Pb, the melt dissolves and transports the oxygen on the steel surface and the protective oxide layer based on Me_3O_4 ($\text{Me} = \text{Fe}, \text{Cr}$)

has been formed [14–16]. Both oxides are based on magnetite structure: the inner layer is (Fe- and Cr-) enriched oxide $(\text{Fe,Cr})_3\text{O}_4$ (spinel type), whereas the outer layer is Cr-depleted Fe_3O_4 .

As it follows from Figure 2 that the outer layer containing Fe and O grows from the initial "solid metal/liquid metal" interface towards the melt, whereas the inner oxide layer, enriched in Cr, grows towards the matrix. This result is in good accordance with those obtained for conventional steels [17]. Figure 6 clearly illustrates the separation between Fe_3O_4

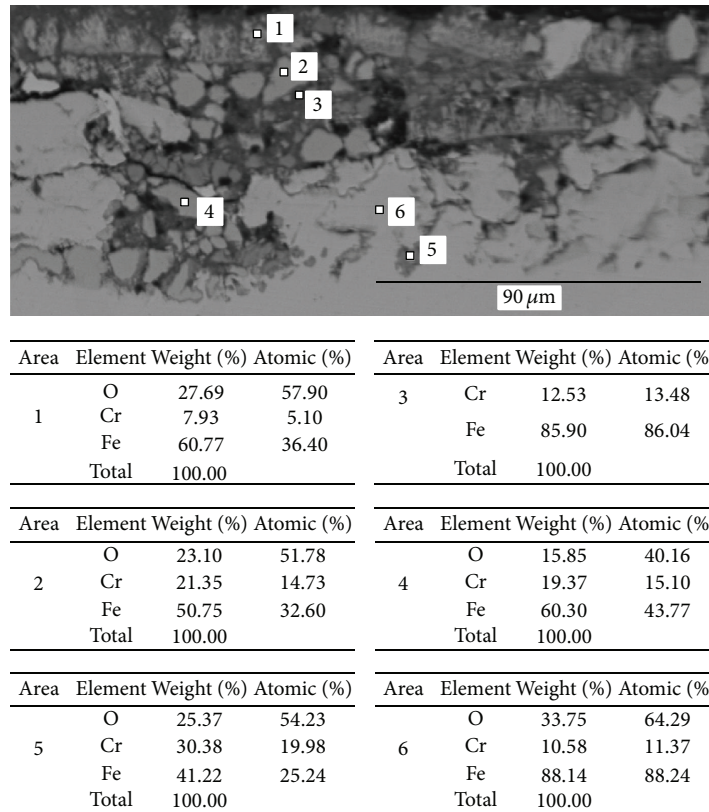


FIGURE 5: Morphology and elemental amount of scales formed on ODS Fe-14Cr steel after exposure to static oxygen-saturated Pb-melt at 550°C for 1000 h.

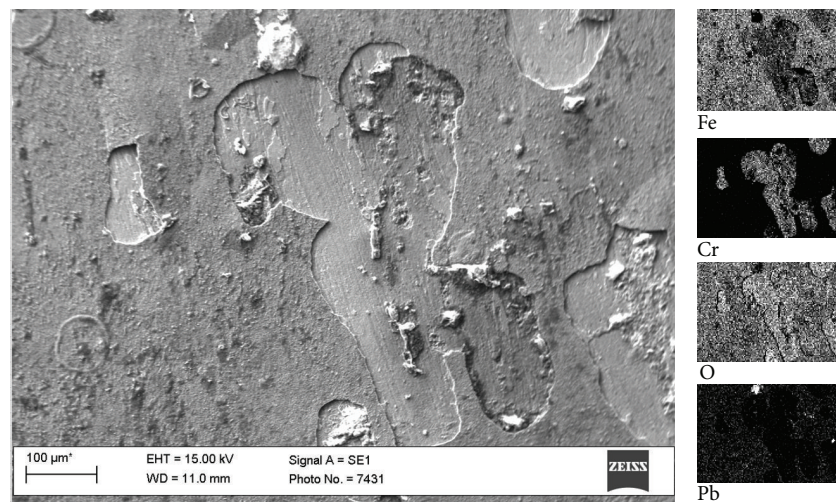


FIGURE 6: Surface morphology (SEM) and composition of ODS Fe-9Cr steel after exposure to oxygen-saturated Pb melt at 550°C for 240 h.

and $(\text{Fe,Cr})_3\text{O}_4$ on the surface of Fe-9Cr steel. After 500 h of exposure, the Cr-depleted Fe_3O_4 layer is separated from $(\text{Fe,Cr})_3\text{O}_4$ (Figure 7).

The increase of Cr amount in ODS steel does not change the regularity of scale formation. After initial period of exposure of ODS Fe-14Cr steel to oxygen-saturated Pb melt for 240 h, the composition of scale is based on

$(\text{Fe,Cr})_3\text{O}_4$ (Figure 8(a)), while with the prolonged exposure of 500 h, the magnetite Fe_3O_4 -based scale is formed (Figure 8(b)).

The informative fragment of surface of ODS Fe-14Cr steel after exposure for 1000 h presented in Figure 9(a) allows three-layered scale to be revealed. The surface is nonuniform. It is possible to distinguish the protrusions of

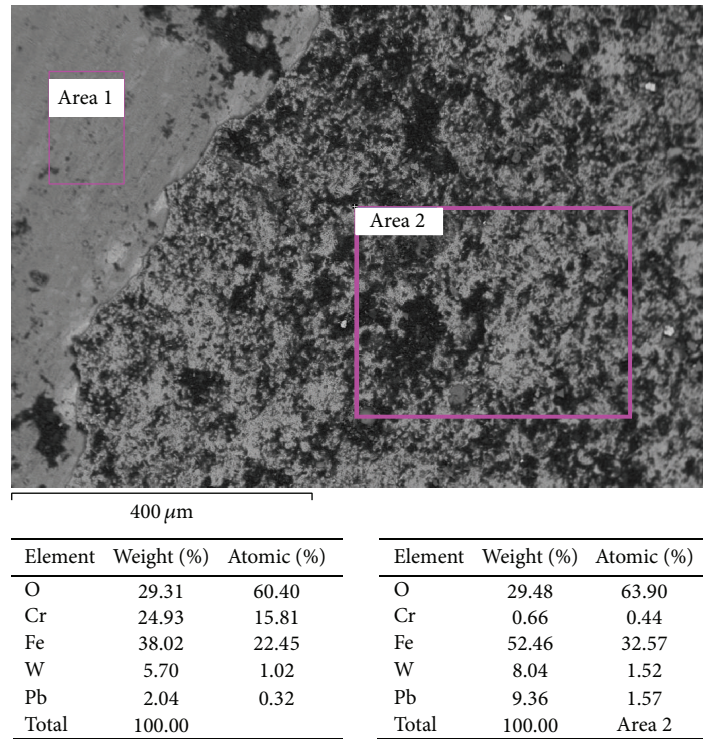


FIGURE 7: Surface morphology (SEM) and composition of ODS Fe-9Cr steel after exposure to oxygen-saturated Pb melt at 550°C for 500 h.

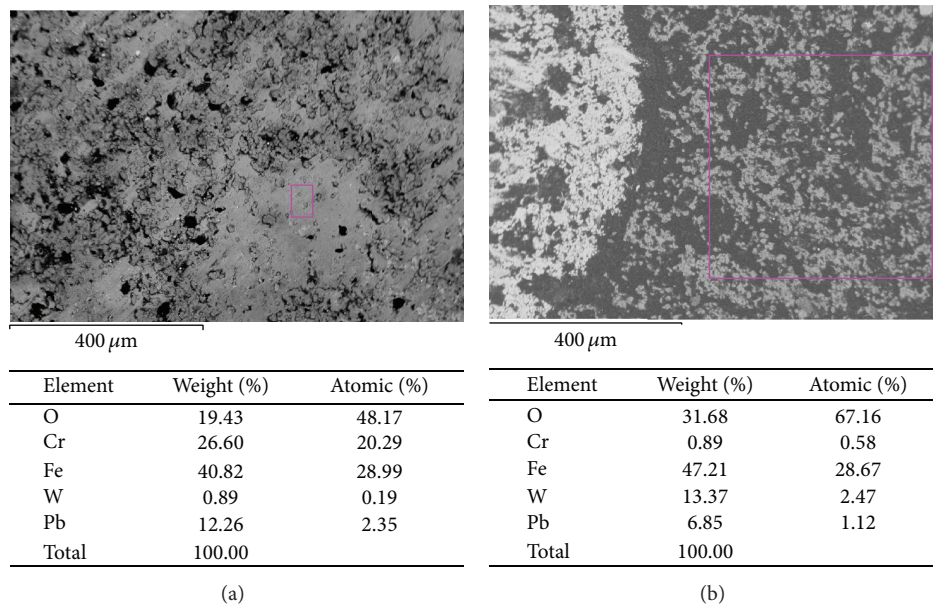
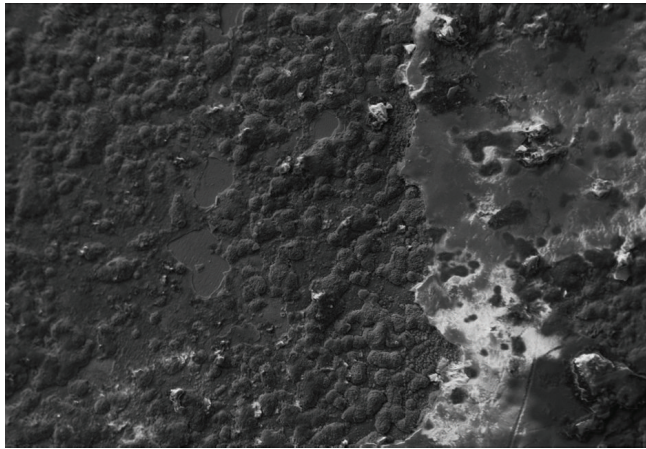


FIGURE 8: Surface morphology (SEM) and composition of ODS Fe-14Cr steel after exposure to oxygen-saturated Pb melt at 550°C for 240 h (a) and 500 h (b).

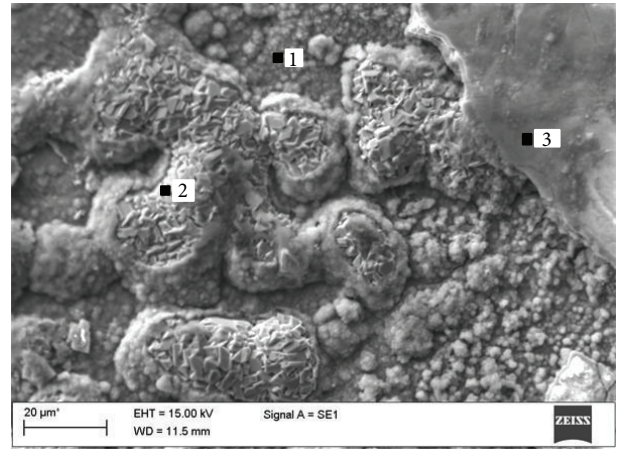
oxide crystals formed on the inner continuous oxide layer (Figure 9(b)). Local energy-dispersive X-ray spectroscopy analysis performed with higher magnification indicates that protrusions are composed of Fe and O (Figure 9(b), area 2), while the continuous inner oxide sublayer (Figure 9(b), area 1) is enriched in Cr. The outer layer is also composed of Fe_3O_4 (Figure 9(b), area 3). It can be presumed that the Fe_3O_4 layer

is growing on the preliminarily formed $(\text{Fe,Cr})_3\text{O}_4$ or even Cr-based (Cr_2O_3) oxide layer and this confirms the above-mentioned assumptions.

Taking into account the structure of oxide layers formed on both Fe-9Cr and Fe-14Cr ODS steels exposed to oxygen-saturated Pb melt at 550°C, the following mechanism of oxidation can be presumed (Figure 10). Initially, the Cr-rich



400 μm



Element	Weight (%)	Atomic (%)	Element	Weight (%)	Atomic (%)
O	20.29	49.19	O	27.56	58.86
Cr	19.63	14.64	Cr	0.78	0.51
Fe	48.70	33.82	Fe	64.45	39.43
W	0.36	0.08	W	0.23	0.04
Pb	10.69	2.00	Pb	6.99	1.15
Total	100.00	Area 1	Total	100.00	Area 2

Element	Weight (%)	Atomic (%)
O	35.66	67.30
Cr	0.69	0.40
Fe	58.27	31.51
W	0.30	0.05
Pb	5.08	0.74
Total	100.00	Area 3

(a)

(b)

FIGURE 9: Surface morphology (SEM) and composition of ODS Fe-14Cr steel after exposure to oxygen-saturated Pb melt at 550°C for 1000 h.

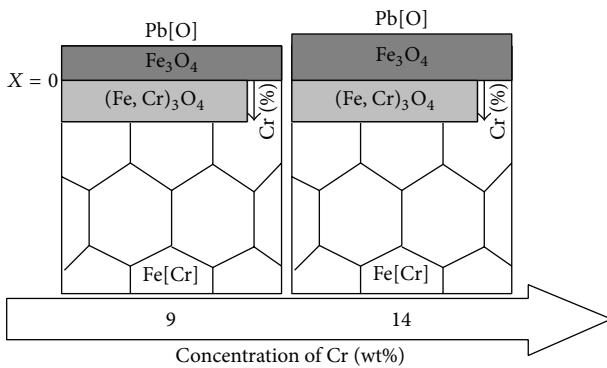


FIGURE 10: Scheme of scale formation of ODS steels.

film grows on the base of the natural oxide film existing on the steel surface before immersion into liquid lead. This continuous Cr_2O_3 -based sublayer protects the steel from the intensive oxidation during some latent period of exposure. With time, when diffusion of chromium cations into the oxide film decreases due to depletion of the suboxide layer in Cr, the iron cations begin to diffuse from the solid metal through the chromium sublayer to liquid metal. Since

the oxidation potential of the melt (10^{-3} wt% O) at 550°C is enough to provide oxidation of Fe, as a result, the pure Fe-based oxides form over the initial Cr-based oxide layer. The growth of the outer magnetite layer is accompanied by the formation of inner spinel enriched in Cr. With the prolongation of exposure, the outer Fe_3O_4 oxide covers the surface uniformly (see Figure 9(b), area 3).

5. Conclusions

The oxidation/corrosion kinetics in static oxygen-saturated Pb melt ($C_{O[Pb]} \sim 10^{-3}$ wt% O) at temperature of 550°C as well as the morphology and composition of oxide scales formed on ferritic/martensitic Fe-9Cr-1.5W ODS and ferritic Fe-14Cr-1.5W ODS steels have been investigated.

Both ODS materials showed homogeneous dense multiple oxide layers that consisted of typical combination of outer Fe_3O_4 and inner $(Fe, Cr)_3O_4$ sublayers. A nonuniform growth of inner oxide sublayer, enriched with Cr, towards the metal matrix is observed in most of the stages of oxidation process. The outer magnetite layer grows toward the melt. No selective oxidation like pitting or grain boundary oxidation was found.

The inner $(\text{Fe,Cr})_3\text{O}_4$ sublayers are mainly well adhered to the metal substrate.

The mechanism of oxidation of ODS steels has been discussed. Primarily, the $(\text{Fe,Cr})_3\text{O}_4$ or even Cr_2O_3 -based layer formed on the surface followed by Fe_3O_4 -based layer.

Kinetics research of corrosion reveals that scale grows more actively on Fe-14Cr steel: from $35\ \mu\text{m}$ to $45\ \mu\text{m}$ for Fe-9Cr ODS steel and from $35\ \mu\text{m}$ to $60\ \mu\text{m}$ for Fe-14Cr ODS steel with exposure prolongation from 240 to 1000 h.

Obtained results indicate that oxidation behavior of ferritic and ferritic/martensitic ODS steels in molten lead corresponds in general to traditional chromium steels when the interaction between steels and lead melt at elevated temperature in static condition results in the formation of a multilayer scale with outer sublayer based on magnetite and inner sublayer based on spinel $(\text{Fe,Cr})_3\text{O}_4$.

Conflict of Interests

The authors declare that there is no conflict of interests regarding the publication of this paper.

Acknowledgment

The present paper was done under the support of IAEA Research Contract no. 16707.

References

- [1] "Design of an Actinide Burning, Lead or Lead-Bismuth Cooled Reactor That Produces Low Cost Electricity," (INEEL/EXT-01-01376. MIT-ANP-PR-083. FY-01 Annual Report, 181, 2001).
- [2] "Comparative assessment of thermophysical and thermohydraulic characteristics of lead, lead-bismuth and sodium coolants for fast reactors," (IAEA-TECDOC-1289, Vienna, 2002).
- [3] "Power reactors and sub-critical blanket systems with lead and lead-bismuth as coolant and/or target material," (IAEA-TECDOC-1348. 2003).
- [4] R. L. Klueh, J. P. Shingledecker, R. W. Swindeman, and D. T. Hoelzer, "Oxide dispersion-strengthened steels: a comparison of some commercial and experimental alloys," *Journal of Nuclear Materials*, vol. 341, no. 2-3, pp. 103–114, 2005.
- [5] K. Ehrlich, E. E. Bloom, and T. Kondo, "International strategy for fusion materials development," *Journal of Nuclear Materials*, vol. 283–287, no. 1, pp. 79–88, 2000.
- [6] U. Shigeharu and M. Fujiwara, "Perspective of ODS alloys application in nuclear environments," *Journal of Nuclear Materials*, vol. 307–311, no. 1, pp. 749–757, 2002.
- [7] V. Kochubey, H. Al-Badairy, G. Tatlock, J. Le-Coze, D. Naumenko, and W. J. Quadackers, "Effects of minor additions and impurities on oxidation behaviour of FeCrAl alloys. Development of novel surface coatings compositions," *Materials and Corrosion*, vol. 56, no. 12, pp. 848–853, 2005.
- [8] G. Y. Lai, *High Temperature Corrosion of Engineering Alloys*, ASMInt, Materials Park, Ohio, USA, 1990.
- [9] K. Kikuchi, *Comprehensive Nuclear Materials 207*, 2012.
- [10] L. Soler, F. J. Martín, F. Hernández, and D. Gómez-Briceño, "Corrosion of stainless steels in lead-bismuth eutectic up to 600°C ," *Journal of Nuclear Materials*, vol. 335, no. 2, pp. 174–179, 2004.
- [11] J. Zhang and N. Li, "Analysis on liquid metal corrosion-oxidation interactions," *Corrosion Science*, vol. 49, no. 11, pp. 4154–4184, 2007.
- [12] R. Ganesan, T. Gnanasekarana, and R. S. Srinivasab, "Standard molar Gibbs free energy of formation of $\text{PbO}(\text{s})$ over a wide temperature range from EMF measurements," *Journal of Nuclear Materials*, vol. 320, no. 3, pp. 258–264, 2003.
- [13] *Handbook on Lead-Bismuth Eutectic Alloy and Lead Properties, Materials Compatibility, Thermohydraulics and Technologies*, 2007.
- [14] N. Li, "Active control of oxygen in molten lead-bismuth eutectic systems to prevent steel corrosion and coolant contamination," *Journal of Nuclear Materials*, vol. 300, no. 1, pp. 73–81, 2002.
- [15] V. M. Fedirko, O. I. Eliseeva, V. I. Kalyandruk, and V. A. Lopushans'kyi, "Corrosion of Armco iron and model Fe-Cr-Al alloys in oxygen-containing lead melts," *Materials Science*, vol. 33, no. 2, pp. 207–211, 1997.
- [16] J. Zhang, "A review of steel corrosion by liquid lead and lead-bismuth," *Corrosion Science*, vol. 51, no. 6, pp. 1207–1227, 2009.
- [17] M. Machut, K. Sridharan, N. Li, S. Ukai, and T. Allen, "Time dependence of corrosion in steels for use in lead-alloy cooled reactors," *Journal of Nuclear Materials*, vol. 371, no. 1–3, pp. 134–144, 2007.



Hindawi

Submit your manuscripts at
<http://www.hindawi.com>

